

SiC-FET Gas Sensor for Detecting Sub-ppm Gas Concentrations

Yoshitaka Sasago^{*1}, Hitoshi Nakamura¹, Takahiro Odaka¹, Atsushi Isobe¹, Shigenobu Komatsu¹, Yohei Nakamura¹, Taizo Yamawaki¹, Chiko Yorita², Nobuyuki Ushifusa², Kohei Yoshikawa³, Kazuo Ono¹, Yumiko Anzai⁴, Shuntaro Machida¹, Masaharu Kinoshita¹, Koji Fujisaki¹, Kenji Okishiro⁵, Yuta Sugiyama⁶

¹Center for Technology Innovation – Electronics, Hitachi, Ltd., Tokyo, 185-8601, Japan

²Center for Technology Innovation – Production Engineering, Hitachi, Ltd., Kanagawa, 244-0817, Japan

³Center for Technology Innovation – Materials, Hitachi, Ltd., Ibaraki, 319-1292, Japan

⁴Center for Technology Innovation – Healthcare, Hitachi, Ltd., Tokyo, 185-8601, Japan

⁵Global Research & Innovative Technology Center *GRI T*, Hitachi Metals, Ltd., Saitama, 360-8577, Japan

⁶Cable Materials Company, Hitachi Metals, Ltd., Ibaraki 319-1418, Japan

ARTICLE INFO

Article history:

Received: 30 September, 2019

Accepted: 23 December, 2019

Online: 22 January, 2020

Keywords:

Capacitor

Platinum

YSZ

Nickel oxide

Nitrogen oxides (NO_x)

Nitrogen monoxide (NO)

Oxygen (O₂)

Sulfur oxide (SO₂)

Carbon monoxide (CO)

Ammonia (NH₃)

ABSTRACT

This paper describes a silicon carbide-field effect transistor (SiC-FET) gas sensor that is able to detect NO, O₂, NH₃, CO, and SO₂. The gate of the sensor FET is a gas detection layer that consists of yttria-stabilized zirconia, nickel oxide, and platinum. The threshold voltages of the sensor depend on the target gas concentration, measurement temperature, and sensor gate materials. The device on SiC substrate can measure gas at temperatures up to 800°C. The gate material dependence and the wide-range temperature dependence of the sensitivity make it possible to detect the concentration of each component in a mixture of gases. In addition, a gate stack composed of composite materials improves the sensitivity of the FET sensor by helping to maintain the sensor's heat resistance and the reproducibility of its measurements.

1. Introduction

In particular, pollution in the atmosphere directly affects human health. Here, nitrogen oxides (NO_x) are the most harmful components of automobile exhaust gas, and sensitive gas sensing is required for detecting them. In Ref. [1], we developed an SiC-FET-type NO_x sensor for high-temperature exhaust gas with a sub-ppm nitrogen monoxide (NO) detection capability.

Limiting-current-type [2], mixed-potential-type [3], and resistive-type [4] sensors have been developed for NO_x detection.

^{*}Yoshitaka Sasago, 1-280 Higashi-Koigakubo, Kokubunji, Tokyo 185-8601, Japan, +81-42-323-1111 & yoshitaka.sasago.tx@hitachi.com

The limiting-current type detects the electric current generated by oxygen ions from NO when a voltage is applied, and the oxygen-ion current depends on the NO concentration. This sensor can detect NO in a wide range of concentration, and it has been used in cars with diesel engines. The mixed-potential type detects voltages produced by NO_x. The resistive type detects current flowing through gas-detection materials under an applied voltage. Compared with the limiting-current and resistive types, the SiC-FET sensor does not need a current to flow through the gas detection materials, because the current flows on the surface of the SiC. Furthermore, since the SiC-FET amplifies the gas-sensing signals, it is more sensitive than the mixed-potential type [3].

The SiC-FET NO_x sensor can detect NO in the mixture of gases in exhaust fumes when it is equipped with an ion-pumping device for preprocessing. The ion-pumping device can remove disturbance gases, and thereby, it enhances the selectivity of the sensor for NO gas [2, 5]. Moreover, without the on-chip ion-pumping device, the sensor can detect several gases such as oxygen (O₂), sulfur oxide (SO₂), carbon monoxide (CO), and ammonia (NH₃). These gases are also included in the exhaust from automobile engines. Instead of improving the sensor's selectivity by removing disturbance gases, we propose that it can be enhanced by using the temperature dependence of gas sensitivity. The high-temperature immunity of SiC-FETs suggests that they can be used for gas-sensing operation over a wide range of temperatures, and the sensitivity to each gas component of these devices varies depending on the sensing temperature.

In this study, we examined the temperature dependence of the gas responses of the SiC-FET sensor. We found that it can sensitively detect several different gases at high temperature. We conclude that a low-cost gas sensor with high sensitivity can be realized by taking advantage of semiconductor products.

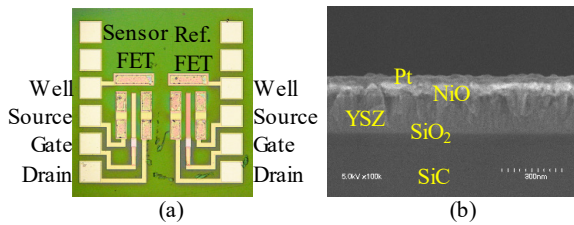


Figure 1: SiC-FET-type NO_x sensors [1]: (a) photograph of SiC chip (2 mm × 2 mm), (b) gate layer of sensor FET.

2. Device Structure and Operation Principle

As shown in Fig. 1(a), the SiC-FET NO_x sensor chip measuring 2 × 2 mm² includes a sensor FET, a reference FET, and platinum electrodes for the well, source, gate, and drain terminals on the edges on both sides [1]. Both FETs have a gate layer stack of yttria-stabilized zirconia (YSZ), nickel oxide (NiO), and platinum (Pt) on a gate oxide layer (Fig. 1 (b)). The platinum layer of the sensor FET is exposed to the atmosphere, while that of the reference FET is covered with dielectric films. The composition of YSZ is (ZrO₂)_{0.97}(Y₂O₃)_{0.03}. The process flow of the sensor chip is explained in Ref. [1]. Since NO, O₂, SO₂, CO, and NH₃ can only be sensed at high temperature, a heater should be placed near the sensor. The heater can be included in a module along with the sensor.

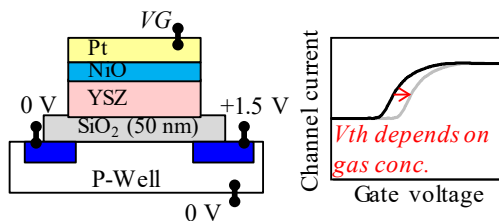


Figure 2: Device structure and operation principle of FET-type sensor [1].

The operation principle of the SiC-FET gas sensor is described in Ref. [1]. As shown in Fig. 2, the threshold voltage (V_{th}) of the sensor FET shifts by increasing the target gas concentration. For example, when the target gas is NO, V_{th} shifts in the positive direction as the concentration increases. However, V_{th} shifts in the

negative direction for NH₃. The target gas concentration can be calculated from the V_{th} shift. A SiC-FET gas sensor was studied for hydrogen detection [6] and ammonia detection [7], but its gate structure was different from our device. The gate material can facilitate detection of target gases. The FET- and capacitor-type gas sensors are classified as work function-type sensors [8].

3. Gas Detection Material

FET sensors have been studied for detection of hydrogen [6, 9–10], ammonia [7], oxygen [11], NH₃ and H₂S [12], etc. The gate layers of these sensors consist of detection materials, which determine the gas detection characteristics of the sensors. Here, we examined the oxygen gas response of the sensor because our primary targets are oxygen-related gases. To select suitable gate-layer materials, we compared the oxygen gas response of the SiC-FET gas sensors with those of Si-FET gas sensors.

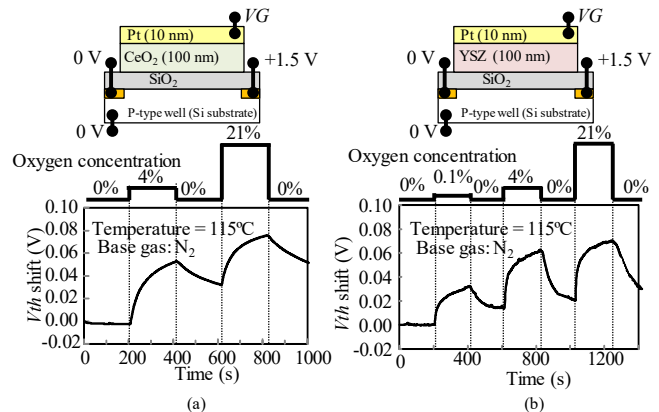


Figure 3: Oxygen gas response characteristics of Si-FET-type gas sensor: (a) platinum-ceria gate, (b) platinum-YSZ gate.

The oxygen response characteristics of the sensors with a platinum-YSZ gate and a platinum-ceria gate are compared in Fig. 3. The platinum, ceria, and YSZ films were deposited by sputtering. YSZ and ceria are oxygen ion conductors [13, 14], and platinum is a commonly used electrode for gas sensors [9–12]. Both sensors responded to oxygen gas; V_{th} shifted in the positive direction at 115°C, and the shifts depended on the oxygen concentration.

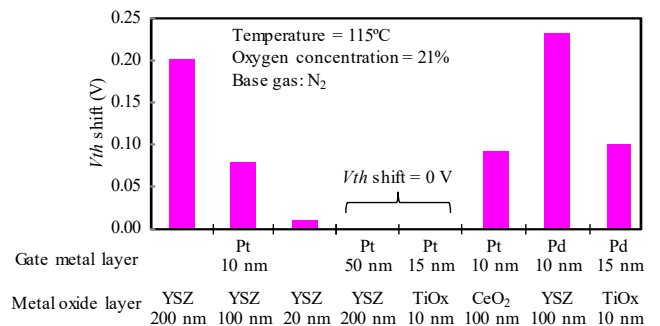


Figure 4: V_{th} shifts of Si-FET-type gas sensors with different gate layer materials.

The V_{th} shifts of different gate-layer materials are summarized in Fig. 4 for 21% oxygen at 115°C. The shifts depended on the thickness of the platinum layer, which is consistent with the results in Ref. [11]. The sensor with 10-nm-thick platinum responded to

oxygen gas, but the one with 50-nm-thick platinum did not. The thickness of YSZ also affected the V_{th} shift. The sensor with 10-nm-thick platinum and 200-nm-thick YSZ responded to oxygen gas. However, V_{th} shift decreased with decreasing YSZ thickness, and the sensor with 20-nm-thick YSZ hardly responded to oxygen gas. Platinum-titania gate FET responded to hydrogen gas, but not oxygen gas [9, 10]. The palladium-titania gate sensor responded to oxygen gas, but the platinum-titania gate sensor did not. The response of the sensor with 10-nm-thick palladium and 100-nm-thick YSZ was the largest of the test samples.

Among the oxide and metal materials in Fig. 4, platinum and YSZ are stable in terms of their chemistry and mechanics. Ceria is reduced in hydrogen atmosphere [14], and palladium is mechanically fragile because its volume expansion and contraction are large under a change in the hydrogen concentration. For these reasons, we selected platinum and YSZ for our SiC-FET gas sensor. The problem is that a thin-film platinum layer does not resist high temperatures over 500°C, while a sensor with a thick platinum layer (50 nm) does not respond to oxygen at 115°C, as shown in Fig. 4. However, a sensor thick platinum layer can do so at higher temperatures, as described below. We decided to use a 100-nm-thick platinum layer.

Although the sensor reported in Ref. [3, 15] is not an FET type, in that study it was shown that a catalytic metal oxide layer helps to enhance sensitivity for NOx [3, 15]. NiO and WO₃ are promising candidates for the catalytic layer, and one made of NiO shows excellent catalytic characteristics. Therefore, we decided to use a NiO layer in our sensor. In particular, NiO layers with thicknesses of 10 nm and 50 nm were formed between the platinum and YSZ layers. Moreover, composite material layers consisting of Pt and NiO were used instead of stacks of NiO and Pt.

The composition of the YSZ film was measured by X-ray photoelectron spectroscopy (XPS). It was the same as that of the sputtering target ((ZrO₂)_{0.97}(Y₂O₃)_{0.03}). No segregation of yttria was observed.

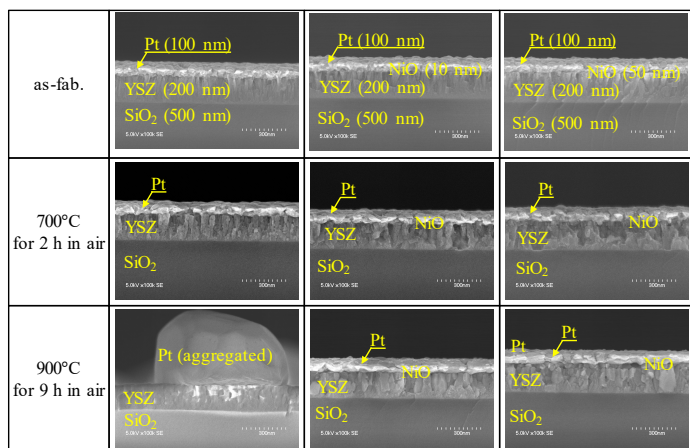


Figure 5: Heat resistance of sensor gates with 100-nm thick platinum. The photographs in the left and central columns are from Ref. [1].

The heat resistance of the gate stacks was examined by taking SEM micrographs. The results for the Pt-YSZ stacks and Pt-NiO-YSZ stacks are shown in Fig. 5. The platinum layer without the NiO layer became aggregated and disconnected at 900°C, but those with the 10-nm-thick and 50-nm-thick NiO layers remained continuous. The results for the stacks with composite material

layers are shown in Fig. 6. The composite material layers also showed heat resistance up to 900°C. These results indicate that gate stacks with NiO could possibly achieve gas sensing at temperatures up to around 900°C.

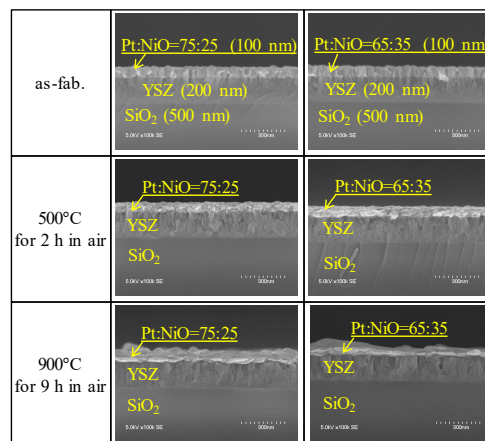


Figure 6: Heat resistance of sensor gates with Pt-NiO composite materials. The photographs in the left columns are from Ref. [1].

4. Gas-Sensing Characteristics

By virtue of the large band gap of SiC, SiC FETs are capable of on- and off-switching at over 500°C; thus, the V_{th} shift of the SiC-FET gas sensor can be detected [1]. On the other hand, switching at 500°C is impossible for Si FETs.

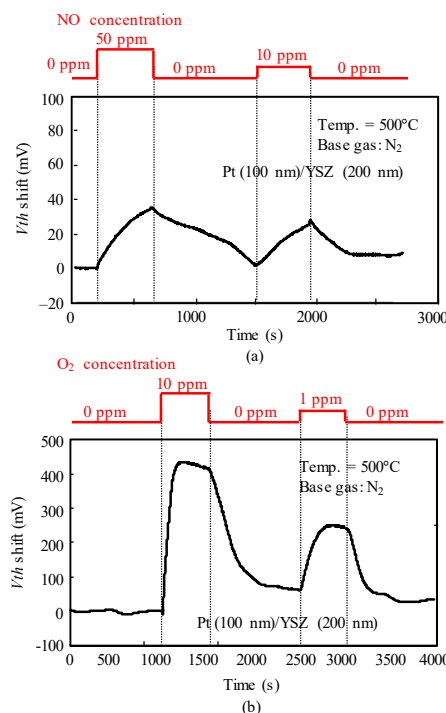


Figure 7: Gas response characteristics of the SiC-FET-type gas sensor with Pt-YSZ gate: (a) NO response, (b) O₂ response.

The time dependence of V_{th} was measured for the SiC-sensor FET. As Figs. 7 and 8 show, V_{th} depended on the concentrations of NO and O₂. Moreover, as shown in Fig. 7, the sensor with the Pt-YSZ gate responded to both NO and O₂, but its sensitivity to O₂

was higher. It clearly responded to 1 ppm O₂, with a *V*_{th} shift of about 250 mV, and it responded to 10 ppm NO with a *V*_{th} shift of about 25 mV. As well, the Pt-NiO-YSZ gate FET responded to both NO and O₂. The *V*_{th} shift for 1 ppm O₂ was about 200 mV, and that for 10 ppm NO was about 75 mV. The selectivity for NO and O₂ was thus modified by inclusion of the NiO layer.

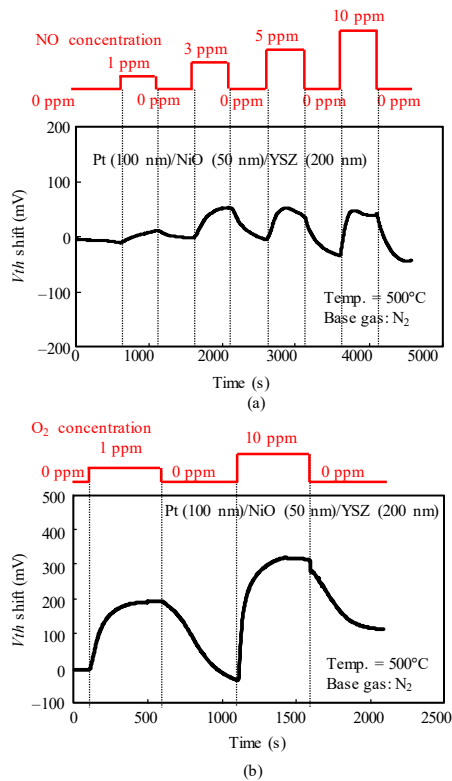


Figure 8: Gas response characteristics of the SiC-FET-type gas sensor with Pt-NiO-YSZ gate [1]: (a) NO response, (b) O₂ response.

We fabricated SiC-FET sensors on SiC wafers and measured the gate-length dependence of the FET characteristics of seven samples in air. In particular, *V*_{th} of the FET decreased smoothly as the gate length decreased; therefore, the sample variation was small. However, the gas response characteristics were measured in only one sample with a gate length of 100 nm for the sensor with the Pt-YSZ gate and the one with the Pt-NiO-YSZ gate. The sample-to-sample variation of gas responses thus remains an issue for future study.

Because of the sample variation problem, we decided to measure the responses of MOS-capacitor-type sensors with N-type SiC substrates instead for NO, O₂, SO₂, CO, and NH₃. While MOS capacitors are simpler than FETs, a change in the target gas concentration produces *V*_{th} shifts in these sensors like in FET sensors. Both FET- and capacitor-type gas sensors are classified as work function-type sensors [8].

As shown in Fig. 9, *V*_{th} of the Pt-YSZ gate capacitor increased as the concentration of NO gas increased, like the response of the FET sensor shown in Fig. 7(a). We measured the responses of a Pt-NiO-YSZ gate capacitor with 10-nm-thick NiO for NO gas at 700 and 800°C (Fig. 10) and those of a gate capacitor with 50-nm-thick NiO layer for NO gas at 600 and 800°C (Fig. 11). As Fig. 11

(a) shows, the sensor with 50-nm-thick NO layer responded to 0.5-ppm NO at 600°C, and the shift for 50 ppm NO was larger than 300 mV. Comparing Fig. 9 with Fig. 11 (a) suggests that the NiO layer appears to improve the NO sensitivity of the sensor. We also measured the NO responses of the capacitor-type sensor at 400°C, but the sensor hardly responded.

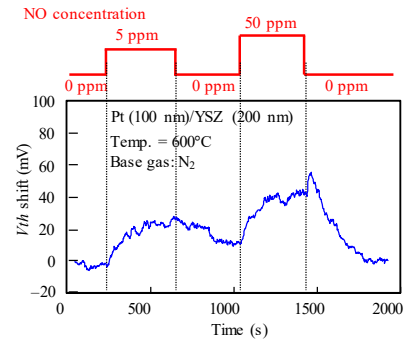


Figure 9: NO response characteristics of SiC-capacitor-type gas sensor with Pt-YSZ gate.

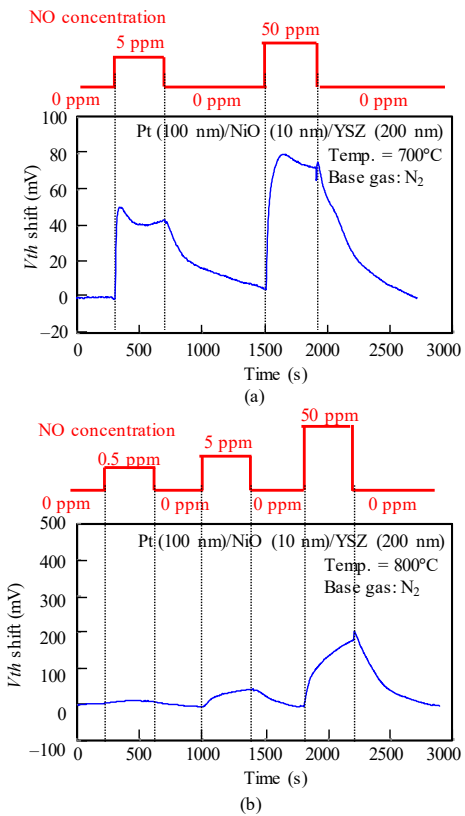


Figure 10: NO response characteristics of SiC-capacitor-type gas sensor with Pt-NiO (10 nm)-YSZ gate: (a) 700°C, (b) 800°C.

We measured the sensor responses of a Pt-YSZ gate capacitor for O₂ gas at 400 and 600°C and those of a Pt-NiO-YSZ gate capacitor with 10-nm-thick NiO for O₂ gas at 400, 600, and 800°C (Figs. 12 and 13). The sensors responded to an O₂ concentration of 0.1 ppm even at 400°C. The O₂ response could be detected at 400°C, while the NO response could not, because the catalytic reaction of the gate layers for O₂ is more active than for NO at low temperatures.

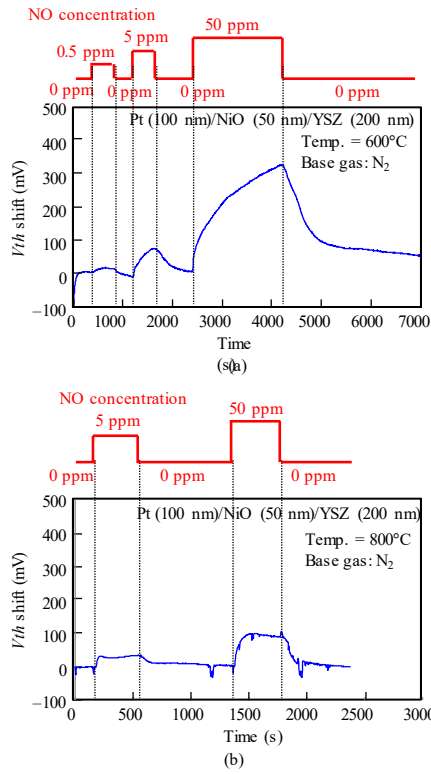


Figure 11: NO response characteristics of SiC-capacitor-type gas sensor with Pt-NiO (50 nm)-YSZ gate: (a) 600°C, (b) 800°C.

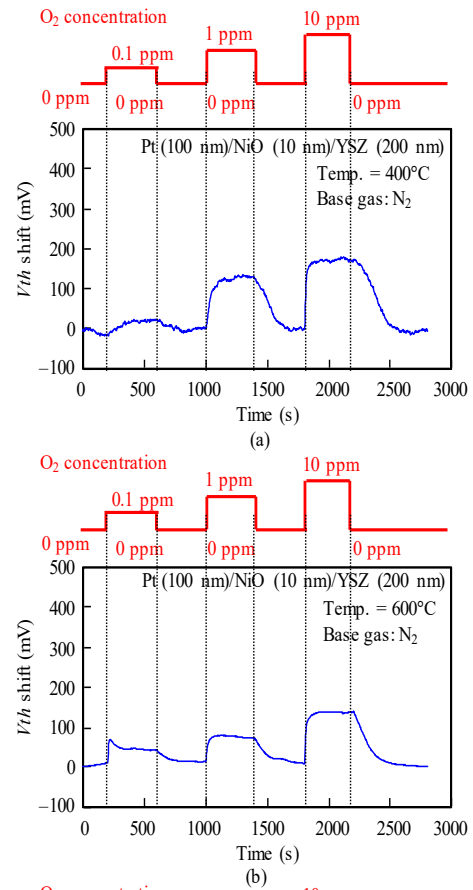


Figure 13: O₂ response characteristics of SiC-capacitor-type gas sensor with Pt-NiO (10 nm)-YSZ gate: (a) 400°C, (b) 600°C, (c) 800°C.

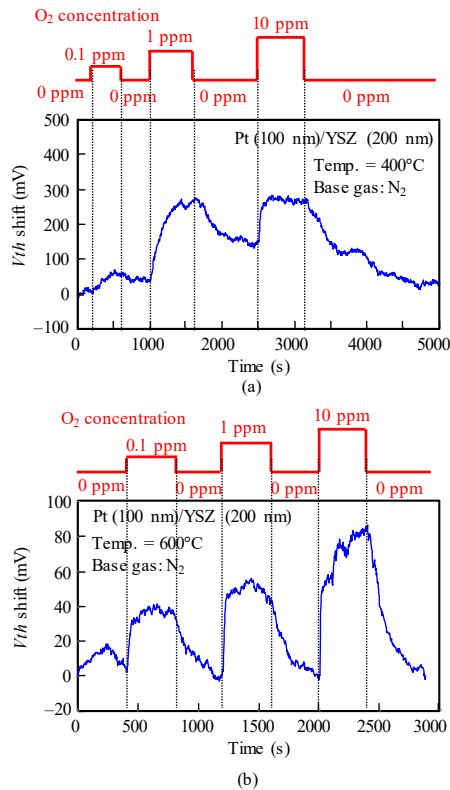


Figure 12: O₂ response characteristics of SiC-capacitor-type gas sensor with Pt-YSZ gate: (a) 400°C, (b) 600°C.

The responses of a Pt-YSZ gate capacitor were measured for NH₃ gas at 400, 600, and 700°C (Fig. 14), and those of a Pt-NiO-YSZ gate capacitor with 10-nm-thick NiO were measured for NH₃ gas at 400, 600, 700, and 800°C (Figs. 15 and 16). Although V_{th} shifted in the positive direction for NO and O₂ (Figs. 7–13), it shifted in the negative direction for NH₃. Note that a negative shift in V_{th} was previously observed in FET-type hydrogen sensors [9, 10]. Both sensors responded to NH₃ of 29 ppm concentration at 400°C. At 700°C, the response of the Pt-YSZ gate capacitor dropped rapidly, but that of a Pt-NiO-YSZ gate capacitor with 10-nm NiO decreased only slightly.

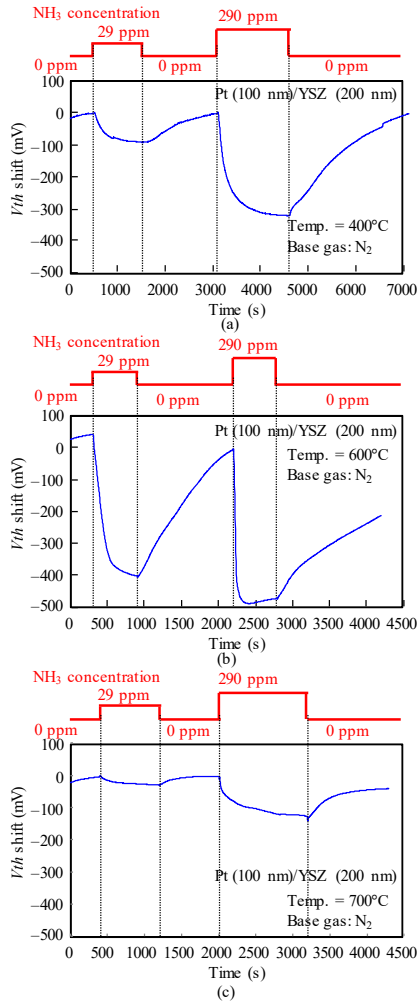


Figure 14: NH₃ response characteristics of SiC-capacitor-type gas sensor with Pt-YSZ gate: (a) 400°C, (b) 600°C, (c) 700°C.

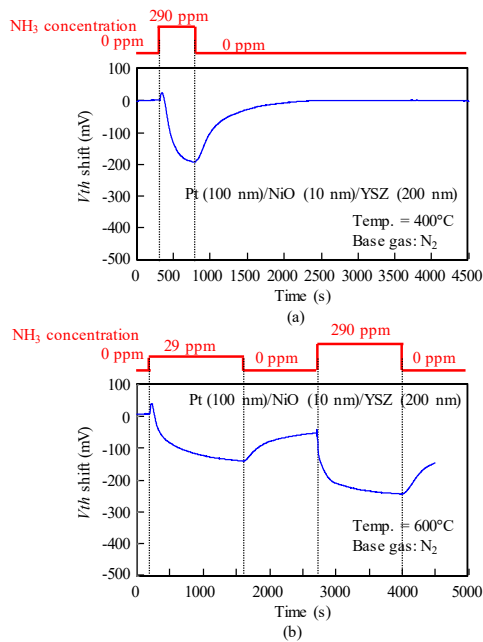


Figure 15: NH₃ response characteristics of SiC-capacitor-type gas sensor with Pt-NiO (10 nm)-YSZ gate: (a) 400°C, (b) 600°C.

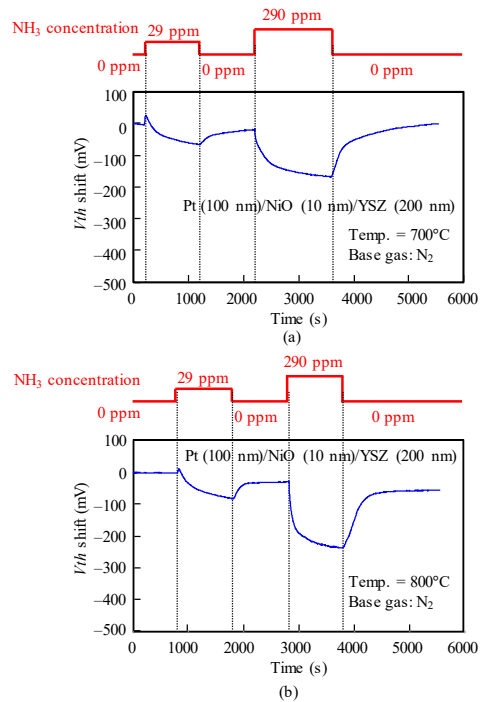


Figure 16: NH₃ response characteristics of SiC-capacitor-type gas sensor with Pt-NiO (10 nm)-YSZ gate: (a) 700°C, (b) 800°C.

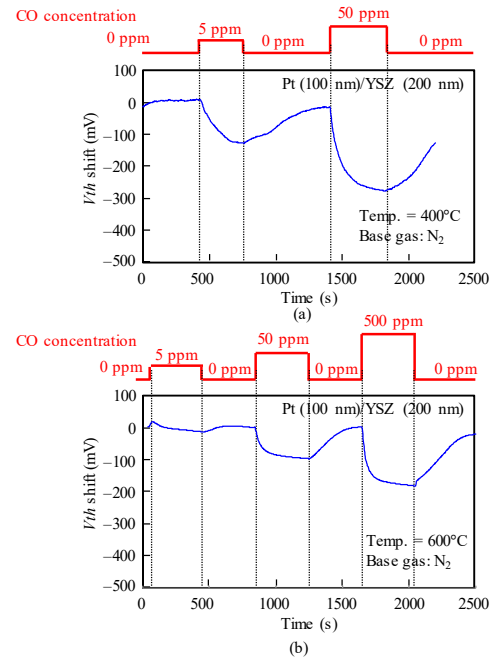


Figure 17: CO response characteristics of SiC-capacitor-type gas sensor with Pt-YSZ gate: (a) 400°C, (b) 600°C.

The sensor responses of the Pt-YSZ gate capacitor were measured for CO gas at 400 and 600°C (Fig. 17) and those of the Pt-NiO-YSZ gate capacitor with 10-nm-thick NiO were also measured for CO gas at 400, 600, and 700°C, as shown in Fig. 18. Similar to the responses for NH₃, V_{th} shifted in the negative direction for CO. The sensors responded to a CO concentration of a 5 ppm at 400°C. As the temperature increased, the sensor response of the capacitors decreased. The Pt-NiO-YSZ gate capacitor was measured at 800°C, but it did not respond to CO gas.

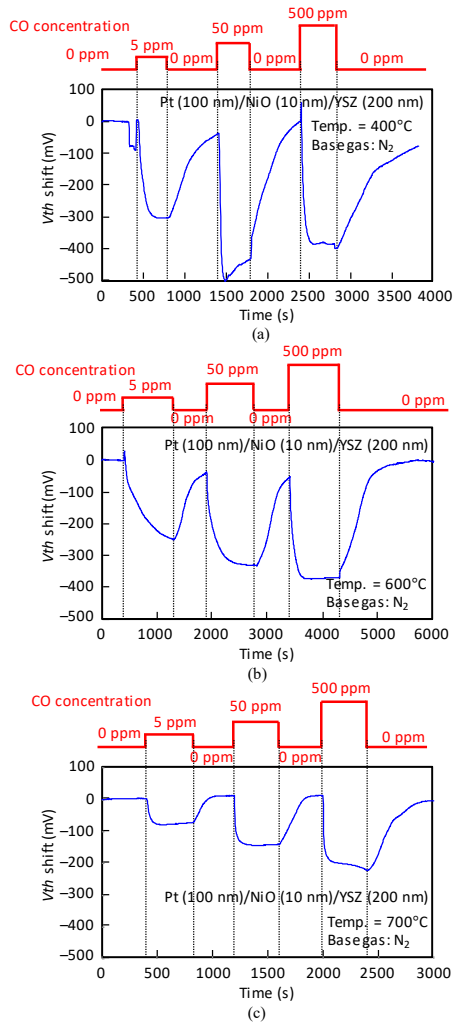


Figure 18: CO response characteristics of SiC-capacitor-type gas sensor with Pt-NiO (10 nm)-YSZ gate: (a) 400°C, (b) 600°C, (c) 700°C.

We measured the sensor responses of a Pt-NiO-YSZ gate capacitor with 50-nm-thick NiO for SO₂ gas at 600 and 800°C. As shown in Fig. 19, *V_{th}* shifted in the positive direction for SO₂ gas, as in the case of NO and O₂ gases. The sensor responded to a 5 ppm concentration of SO₂ at 600°C, and the response slightly decreased at 800°C.

The temperature dependence of the *V_{th}* shifts are summarized in Fig. 20 for NO (5 ppm), O₂ (1 ppm), NH₃ (29 ppm), CO (5 ppm), and SO₂ (5 ppm) gases. The results clearly show that the sensitivity depends on the measurement temperatures and the composition of the gate stack layer. Moreover, the measurement temperature can be controlled by the heater attached to the sensor module. Overall, the results indicate that measurement is possible over a range from 400 to 800°C, which is impossible for Si FET sensors.

The sensor responses of a Pt-YSZ gate capacitor and a Pt-NiO-YSZ gate capacitor were measured at room temperature, but no *V_{th}* shift was observed for NO (5 ppm), O₂ (1 ppm), NH₃ (29 ppm), CO (5 ppm), or SO₂ (5 ppm) gases. These results indicate our sensors have threshold temperatures for gas detection. Similar results are reported for NH₃ and H₂S in Ref. [12], in which the gas response was observed above 200°C for H₂S at a concentration of 400 ppm and above 110°C for NH₃ at a concentration of 500 ppm.

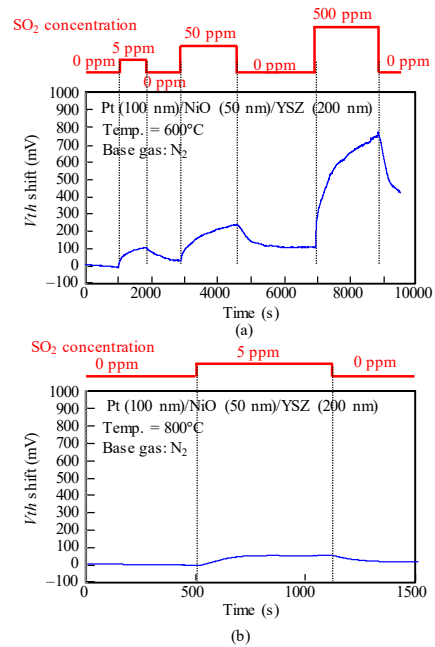


Figure 19: SO₂ response characteristics of SiC-capacitor-type gas sensor with Pt-NiO (50 nm)-YSZ gate: (a) 600°C, (b) 800°C.

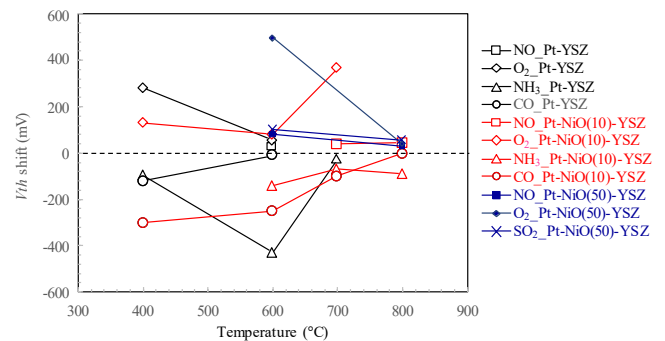


Figure 20: Temperature dependence of *V_{th}* shifts for NO (5 ppm), O₂ (1 ppm), NH₃ (29 ppm), CO (5 ppm), and SO₂ (5 ppm) gases.

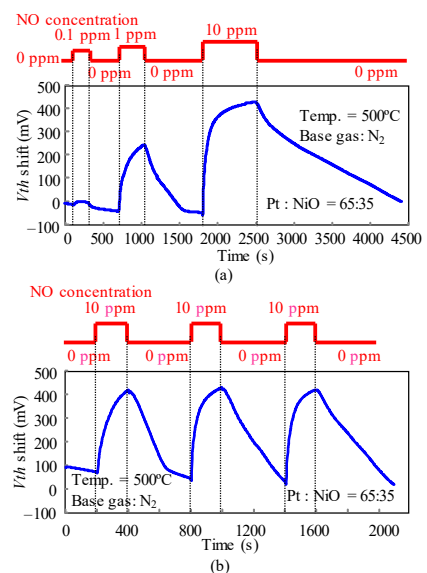


Figure 21: NO response characteristics of SiC-capacitor-type gas sensor with Pt-NiO-composite-material gate: (a) concentration dependence [1], (b) reproducibility.

To increase the sensitivity of the FET-type sensor, the three-phase boundary of the gate should be increased [16]. The nanoporous structure of the gate helps to improve the sensor sensitivity [9, 10]. The sensor with a NiO-Pt composite material gate showed NO detection with 0.1 ppm (Fig. 21 (a)). The reproducibility of the measurements was confirmed for 10 ppm NO₂, as shown in Fig. 21 (b). As mentioned above and as shown in Fig. 6, this sensor was very heat resistant.

5. Conclusion

We developed a SiC-FET-type gas sensors and SiC-capacitor-type gas sensors with a gate stack including YSZ, nickel oxide and platinum. These sensors are able to detect NO, O₂, NH₃, CO, and SO₂. To study the feasibility of the gas detection of each component in the gas mixture, we examined the temperature dependence of the gas response characteristics for each gas.

The nickel oxide layer enhances the heat resistance of the gate stack, and, thus, it extends the range of gas detection temperatures up to 800°C. The nickel oxide layer also helps enhance the sensitivity for NO detection. The sensors successfully detected NO at a concentration of 0.1 ppm. They were also able to respond to O₂ at a concentration of 0.1 ppm.

The gas response characteristics of capacitor-type sensors were measured for NO, O₂, NH₃, CO, and SO₂. The results show that V_{th} shifts in the positive direction for NO, O₂, and SO₂, but shifts in the negative direction for NH₃ and CO. The temperature dependence of the sensitivity was measured at room temperature and from 400 to 800°C. Gas responses were not observed at room temperature, and the sensitivity and the selectivity depended on the measurement temperature and the gate material of the sensors. This results indicate that the concentrations of each gas component can be determined using these dependences. In the future, we will study the sample variation of the gas responses characteristics and derive quantitative formulae for the concentration of each gas component.

In addition to the sensor with a gate stack of YSZ, NiO and Pt, the sensor with a NiO-Pt composite material gate was fabricated, and it was able to detect NO with a concentration of 0.1 ppm. This sensor was heat resistant, and its measurements were reproducible.

Conflict of Interest

The authors declare no conflict of interest.

Acknowledgment

The authors gratefully acknowledge Dr. T. Sekiguchi and Dr. H. Kurata of Hitachi, Ltd. for all their encouragement. The authors also thank all the staff of the clean room of Hitachi's R&D group for the device fabrication. The authors thank Dr. R. Goto, Dr. H. Sano, Dr. T. Shimada, Mr. K. Kato, Mr. N. Ashizuka, and Mr. Y. Nozawa of Hitachi Metals, Ltd. for insightful discussion from the early stage of the research. The authors also thank Mr. Y. Nagai of TOMOE SHOKAI Co., LTD. for valuable assistance with the gas response experiments.

References

- [1] Y. Sasago et al., "SiC-FET-type NO_x Sensor for High-Temperature Exhaust Gas," 2018 IEEE International Electron Devices Meeting, 12.5.1–12.5.4.
- [2] N. Kato, K. Nakagaki, and N. Ina, "Thick Film ZrO₂ NO_x Sensor," SAE Technical Paper 960334 (1996).

- [3] N. Miura et al., "Improving NO₂ Sensitivity by Adding WO₃ during Processing of NiO Sensing-Electrode of Mixed-Potential-Type Zirconia-Based Sensor," *J. Electrochem. Soc.* **154**, pp. 1246–1252 (2007).
- [4] A. Groß et al., "Dual Mode NO_x Sensor: Measuring Both the Accumulated Amount and Instantaneous Level at Low Concentrations," *Sensors* **12**, pp. 2831–2850 (2012).
- [5] T. Inaba and T. Saji, "Low temperature operation of thin-film limiting-current type oxygen sensor using graded-composition layer electrodes," *Sensors and Actuators B* **129**, pp. 874–880 (2008).
- [6] R. Loloee et al., "Hydrogen monitoring for power plant applications using SiC sensors," *Sensors and Actuators B* **129**, 200–210 (2008).
- [7] H. Wingbrant et al., "Using a MISiC-FET Sensor for Detecting NH₃ in SCR Systems," *IEEE Sensors Journal* **5**, pp. 1099–1105 (2005).
- [8] T. Hübert et al., "Hydrogen sensors – A review," *Sensors and Actuators B* **157**, pp. 329–352 (2011).
- [9] T. Usagawa and Y. Kikuchi, "A Pt-Ti-O gate Si-metal-insulator-semiconductor field-effect transistor hydrogen gas sensor," *J. Appl. Phys.* **108**, 074909 (2010).
- [10] Y. Sasago et al., "FET-type hydrogen sensor with short response time and high drift immunity," *Symp. on VLSI Technol.* 2017, T106–T107.
- [11] Y. Miyahara, K. Tsukada, and H. Miyagi, "Field-effect transistor using a solid electrolyte as a new oxygen sensor," *J. Appl. Phys.* **63**, 2431 (1988).
- [12] T. Usagawa and Y. Sasago, "Hydrogen-Related Gas Response from Pt-Ti-O Gate Si-MISFETs Gas Sensors," *Proceedings of the 62nd Chemical Sensor Symposium* **31**, pp. 16-17 (2017).
- [13] S. J. Skinner and J. A. Kilner, "Oxygen ion conductors," *Materials Today* **6**, pp. 30–37 (2003).
- [14] Y. Zhang et al., "Recent Progress on Advanced Materials for Solid-Oxide Fuel Cells Operating Below 500°C," *Adv. Mater.* **29**, 1700132 (2017).
- [15] A. Hemberga et al., "Effect of the thickness of reactively sputtered WO₃ submicron thin films used for NO₂ detection", *Sensors and Actuators B* **171**, pp. 18-24 (2012).
- [16] B. Wang et al., "Fabrication of Well-Ordered Three-Phase Boundary with Nanostructure Pore Array for Mixed Potential-Type Zirconia-Based NO₂ Sensor," *ACS Appl. Mater. Interfaces*, **8**, pp. 16752–16760 (2016).